

# Multiphase Hydrodechlorination of 1,3,5-Trichlorobenzene on Palladium Catalysts Supported on Alumina: Effect of the Support Properties and Modification by Heteropoly Acid Based on Silicon and Tungsten

E. V. Golubina<sup>a</sup>, E. S. Lokteva<sup>a, \*</sup>, U. D. Gurbanova<sup>b</sup>, A. N. Kharlanov<sup>a</sup>, T. B. Egorova<sup>a</sup>, I. A. Lipatova<sup>c</sup>, M. S. Vlaskin<sup>c</sup>, and E. I. Shkol'nikov<sup>c</sup>

<sup>a</sup>Faculty of Chemistry, Moscow State University, Moscow, 119991 Russia

<sup>b</sup>Faculty of Chemistry, Baku Branch, Moscow State University, Khodzhasan, Baku, AZ 1144 Azerbaijan

<sup>c</sup>Joint Institute for High Temperatures, Russian Academy of Sciences, Moscow, 125412 Russia

\*e-mail: e.lokteva@rambler.ru

Received December 10, 2018; revised January 11, 2019; accepted January 15, 2019

**Abstract**—Catalytic systems 2 wt % Pd/Al<sub>2</sub>O<sub>3</sub> were prepared using noncalcined boehmite (NC) and two types of alumina support: one was prepared by the calcination of boehmite at 600°C (C) and the other produced by Engelhard (E). To prepare 2 wt % Pd/HPC–Al<sub>2</sub>O<sub>3</sub> samples, these supports were modified by impregnation by a heteropoly compound (HPC) (20 wt % H<sub>8</sub>[Si(W<sub>2</sub>O<sub>7</sub>)<sub>6</sub>] · 6H<sub>2</sub>O). The effect of the Al<sub>2</sub>O<sub>3</sub> structure and its modification by the heteropoly compound on the physicochemical properties, activity, selectivity and stability of catalysts in the reaction of multiphase hydrodechlorination of 1,3,5-trichlorobenzene (TCB) was studied. All catalysts showed activity in the considered reaction with the predominant formation of benzene but were deactivated in the reaction medium. Modification by the heteropoly compound resulted in increased stability and was especially effective for catalyst supported on Al<sub>2</sub>O<sub>3</sub>(E). The method of scanning electron microscopy (SEM) was used to determine the morphological differences of supports. According to the data of transmission electron microscopy, all catalysts contained palladium in the form of particles less than 20 nm in size. The particle size and width of the size distribution increases in the series Pd/Al<sub>2</sub>O<sub>3</sub>(NC) < Pd/Al<sub>2</sub>O<sub>3</sub>(C) < Pd/Al<sub>2</sub>O<sub>3</sub>(E). Modification by the heteropoly compound was favorable for the decrease in the size of palladium particles. The method of temperature-programmed reduction with hydrogen (TPR-H<sub>2</sub>) showed that all catalysts included in their composition palladium hydride along with more strongly surface-bound metal forms that are reduced at elevated temperatures, and their content decreases after modification by the heteropoly compound and increases after catalytic tests. According to diffuse reflectance infrared Fourier transform spectroscopy (DRIFTS), the deposition of a heteropoly compound leads to a change in the type of Lewis acid sites on the alumina surface and in the electronic state of palladium. According to the results of infrared spectroscopic studies of adsorbed CO, the relatively large particles of Pd<sup>0</sup> are the main form on the surface of nonmodified catalysts. The catalysts modified by the heteropoly compound contain single Pd<sup>+</sup> and Pd<sup>2+</sup> cations, and the fraction of Pd<sup>0</sup> is substantially smaller. The specific features of the Lewis acidity of the catalyst surface determine the possibility of 1,3,5-trichlorobenzene adsorption and activation on the support and the spillover of hydrogen from Pd<sup>0</sup>. An increase in the catalyst stability as a result of support modification by the heteropoly compound can be explained by the appearance of new active sites in the interaction of palladium with the heteropoly compound or its thermal decomposition products.

**Keywords:** palladium, heteropoly acid, alumina, catalyst, hydrodechlorination, 1,3,5-trichlorobenzene

**DOI:** 10.1134/S0023158419030066

## INTRODUCTION

Heterogeneous catalytic hydrodechlorination is an effective way of processing chlorinated organic waste, which is free from the danger of dioxins formation. When utilizing significant amounts of waste, hydrodechlorination makes it possible to isolate and reuse the nonchlorinated part of the molecule, e.g., benzene from chlorobenzenes [1, 2]. The effectiveness of

hydrodechlorination in detoxifying polychlorinated aromatics [1, 3], including polychlorinated dibenzo-*para*-dioxanes/furans (dioxins) [4, 5], water purification from chlorophenols [6, 7], medical products [8–11], and chloroethanes and chloroethylenes [12–14] has been proven. Palladium-containing catalysts [1, 15, 16] turned out to be the most effective and stable, although nonprecious metals—nickel [17], iron [18],

cobalt [19], etc.—are also often used, alone or as part of bimetallic systems with noble components [14, 20, 21]. Adsorption and activation of chlorinated organic compounds can occur both on the metal particles and on the support surface, and the second pathway becomes the main one when the support surface contains Lewis acid sites [16]. In this variant, hydrogen, which is activated on the particles of the active metal by homolytic or heterolytic dissociation is supplied to the molecule adsorbed on the support by the spillover mechanism [16]. Chlorine species and chloride ions formed in hydrodechlorination can cause catalyst deactivation [16] primarily due to the chlorination of the active metal. One approach to limit such deactivation is associated with the introduction of modifying agents, for example, another metal, which reduces the degree of chlorination of the active component [21]. Another promising approach is the modification of support properties. The activity, selectivity, and stability of catalytic systems can be changed by controlling the nature, texture, crystal structure of supports [15, 22].

In this work, in order to change the acidic properties of the surface and prevent the strong interaction of palladium with alumina support, it was modified by introducing a heteropoly compound (HPC) of a silicon and tungsten. Earlier we showed [23] that the modification of the support by adding heteropoly compounds of molybdenum and tungsten can improve the catalytic effect of nickel and palladium–nickel catalysts supported on alumina in chlorobenzene hydrodechlorination by changing the dispersion of the metal and the degree of its interaction with the support. However, the causes of changes occurring upon the modification of supported metal-containing catalysts by heteropoly compounds have been studied insufficiently.

In this work, we study the effect of alumina structure and its modification by  $H_8[Si(W_2O_7)_6] \cdot H_2O$  heteropoly compound on the physicochemical properties, activity, selectivity, and stability of  $Pd/Al_2O_3$  catalysts in hydrodechlorination of 1,3,5-trichlorobenzene in multiphase conditions.

## EXPERIMENTAL

### *Modified Support Preparation*

We used three types of alumina supports: (1)  $Al_2O_3(E)$  is  $\gamma-Al_2O_3$  (Engelhard, USA) with a specific surface area  $S_{BET}$  of  $185 \text{ m}^2/\text{g}$ ; (2)  $Al_2O_3(NC)$  is boehmite prepared by the hydrolysis of aluminum isopropoxide under the action of isopropanol with further drying; (3)  $Al_2O_3(C)$  is  $\gamma-Al_2O_3$  prepared by the calcination of the  $Al_2O_3(NC)$  sample at  $600^\circ\text{C}$ .

The support was modified by the  $H_8[Si(W_2O_7)_6] \cdot 6H_2O$  heteropoly acid (analytical purity grade; Dia-M, Russia) by impregnation. A weighed sample of the support was dried (1 h,  $110^\circ\text{C}$ ) and then wetted with

distilled water. Calculated amount of heteropoly acid solution was added dropwise to the suspension of the carrier with constant stirring (in order to deposit 20 wt % HPS on  $Al_2O_3$ ). After 10 min of further stirring, the suspension was evaporated in a water bath, dried in air for 12 h and then at  $110^\circ\text{C}$  for 1 h and calcined in air (without flowing) for 1 h at  $200^\circ\text{C}$  and then for 3 h at  $400^\circ\text{C}$ . Thus, we obtained three modified supports designated as  $HPC-Al_2O_3(E)$ ,  $HPC-Al_2O_3(NC)$ , and  $HPC-Al_2O_3(C)$ .

### *Catalyst Preparation*

Palladium (2 wt %) was supported on  $Al_2O_3$  by impregnation. A portion of the dry support was wetted with distilled water and stirred for 10 min with a magnetic stirrer. The calculated amount of  $Pd(NO_3)_2$  solution with a palladium content of 10 wt %, a content of nitric acid of 10 wt %, and purity for other metals of 99.999% (Aldrich, USA) was slightly diluted with distilled water and added dropwise to the support suspension with stirring for 10 min. The obtained suspension was stirred for another 10 min, and then evaporated in a water bath, dried in air for 12 h at room temperature and 1 h at  $110^\circ\text{C}$ , and calcined in a static atmosphere in air (rapid heating to  $200^\circ\text{C}$ , allowing to stay for 1 h, then heating to  $400^\circ\text{C}$ , and calcination for 3 h).  $PdO/Al_2O_3$  was reduced in a quartz reactor in a flow of hydrogen (the flow rate of  $H_2$  was  $10 \text{ mL}/\text{min}$ ) at  $500^\circ\text{C}$  for 3 h. After cooling the catalyst to  $50^\circ\text{C}$ , the reactor was purged with nitrogen containing the traces of oxygen for 30 min in order to oxidize the surface of palladium particles and prevent their further oxidation when stored in air.

### *Studies of Catalysts by Physicochemical Methods*

Nitrogen adsorption–desorption isotherms were recorded at 77 K using an Autosorb-1 automated analyzer (Quantachrome, USA). The specific surface area ( $S_{BET}$ ), the pore volume  $V_{\text{pore}}$  and their average diameter  $d_{\text{pore}}$  in the samples were calculated by the BET and BJH methods using the isotherms of nitrogen adsorption–desorption at 77 K using Autosorb software.

Electron microscopic images of the sample surfaces were obtained using a JEOL JSM-6390 scanning electron microscope (JEOL, Japan) equipped with an attachment for local energy dispersive analysis (EDA); the high resolution transmission electron microscopic (HRTEM) images were obtained using a JEM 2100F-UHR instrument (JEOL, Japan) with an attachment for local energy dispersive analysis (EDA) at an accelerating voltage of 200 kV.

Temperature-programmed hydrogen reduction (TPW- $H_2$ ) was carried out on a USGA-101 chemisorption analyzer (Unisit, Russia), passing a 5%  $H_2/Ar$  ( $30 \text{ mL}/\text{min}$ ) mixture through a quartz reactor containing 50 mg of unreduced catalyst precursor with

heating from 30 to 800°C at a rate of 10°C/min. Before analysis, the sample was kept at 300°C for 30 min in a flow of argon and cooled to 30°C. The change in the composition of the gas mixture during the analysis was determined using a thermal conductivity detector. To quantitatively analyze the hydrogen uptake/evolution data, the detector signal was preliminarily calibrated in the TPR-H<sub>2</sub> of standard NiO sample.

Diffuse reflectance infrared spectra were recorded on an EQUINOX 55/S Fourier transform infrared spectrometer (Bruker, Germany). The powder of the sample under study was placed in a quartz ampoule with a CaF<sub>2</sub> window and calcined at 550°C (1 h in air and 2.5 h under vacuum of at most  $5 \times 10^{-5}$  Torr). Gaseous CO was purified by passing through a trap with liquid nitrogen and prolonged aging over calcined zeolite. The differential spectra of adsorbed CO were obtained by subtracting the background spectrum from the experimental spectrum of the sample containing adsorbed CO with the further correction of the baseline in the OPUS 6.0 utility (Bruker).

X-ray diffraction of the samples was carried out on the powder diffractometer STOE STADI-P (STOE & Cie, Germany) using CuK<sub>α</sub> radiation in the range of angles  $2\theta = 10^\circ\text{--}85^\circ$ .

#### *Multiphase Hydrodechlorination of 1,3,5-trichlorobenzene*

The multiphase hydrodechlorination of 1,3,5-trichlorobenzene (TCB) was carried out at 50°C and an atmospheric pressure in a three-neck flask equipped with a thermostated jacket, a magnetic stirrer, a reflux condenser, and a hydrogen supply system. The catalyst

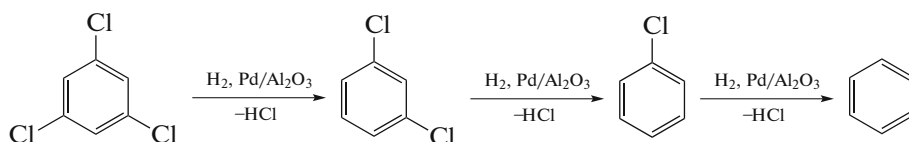
(100 mg) was placed into the reactor heated to a temperature of experiment (50°C). The oxide film was reduced on the surface of palladium particles in a flow of hydrogen (5 mL/min) for 1 h. Then, 3 mL of isooctane and 2 mL of a 0.13 M solution of Aliquat-336 in isooctane were loaded into the reactor and stirred for 5 min and then 6 mL of a 20% aqueous solution of KOH and a solution of 63.6 mg ( $3.5 \times 10^{-4}$  mol) of 1,3,5-trichlorobenzene in 5 mL of isooctane were added. The moment of loading the solution of 1,3,5-trichlorobenzene into the reactor was considered the time of the reaction start. The reaction was carried out with constant stirring and a constant supply of hydrogen at a flow rate of 5 mL/min ( $2.24 \times 10^{-4}$  mol/min).

For the analysis of the reaction mixture, stirring was interrupted and, after layering, the organic phase was sampled. The reaction products were analyzed on an Agilent 6890N gas chromatograph (Agilent, USA; 30-m DB-WAX capillary column with a diameter of 0.25 mm; flame ionization detector).

## RESULTS AND DISCUSSION

### *Catalytic Activity and the Effect of the Reaction Mixture on the Catalyst*

The catalysts obtained in this work were tested in hydrodechlorination of 1,3,5-trichlorobenzene in a multiphase system [24] in a batch reactor at a temperature of 50°C. It is commonly believed that the hydrodechlorination reactions of polychlorinated organic compounds and, in particular, 1,3,5-trichlorobenzene, occur sequentially in accordance with the following scheme:



Figures 1a and 1b show the kinetic curves describing the dependences of the concentrations of the initial 1,3,5-trichlorobenzene and hydrodechlorination products on time in the presence of nonmodified (Fig. 1a) and modified (Fig. 1b) catalysts on the Al<sub>2</sub>O<sub>3</sub>(NC), Al<sub>2</sub>O<sub>3</sub>(C), and Al<sub>2</sub>O<sub>3</sub>(E) supports. It is seen that in all cases, the main product is benzene. Along with 1,3-dichlorobenzene (DCB), it is detected already in the first samples taken 5 min after the start of the reaction. Chlorobenzene (CB) was found in insignificant amounts on nonmodified catalysts and in small amounts on catalysts modified by the heteropoly compound (~1% on Pd/HPC–Al<sub>2</sub>O<sub>3</sub>(C) and ~2% on Pd/HPC–Al<sub>2</sub>O<sub>3</sub>(E)). The concentrations of both intermediates do not pass through the maxima, but rather remain approximately constant throughout

the duration of the reaction. The concentration of 1,3-dichlorobenzene in the reaction mixture is about 12% on the Pd/Al<sub>2</sub>O<sub>3</sub>(C) sample and below 10% on the Pd/Al<sub>2</sub>O<sub>3</sub>(E) catalyst. It is slightly higher in the initial reaction period in the presence of modified systems (~15%), and then noticeably decreases to 10% on the Pd/HPC–Al<sub>2</sub>O<sub>3</sub>(C) sample and to 5% on the Pd/HPC–Al<sub>2</sub>O<sub>3</sub>(E) sample.

Of the three nonmodified catalysts studied, Pd/Al<sub>2</sub>O<sub>3</sub>(NC) is different: the concentration of 1,3-dichlorobenzene and chlorobenzene is approximately the same as for Pd/Al<sub>2</sub>O<sub>3</sub>(C) and Pd/Al<sub>2</sub>O<sub>3</sub>(E), and the benzene concentration is lower, which correlates with the low conversion of chlorobenzene. Modified Pd/HPC–Al<sub>2</sub>O<sub>3</sub>(NC), although it increases the conversion compared to Pd/Al<sub>2</sub>O<sub>3</sub>(NC), is still less active

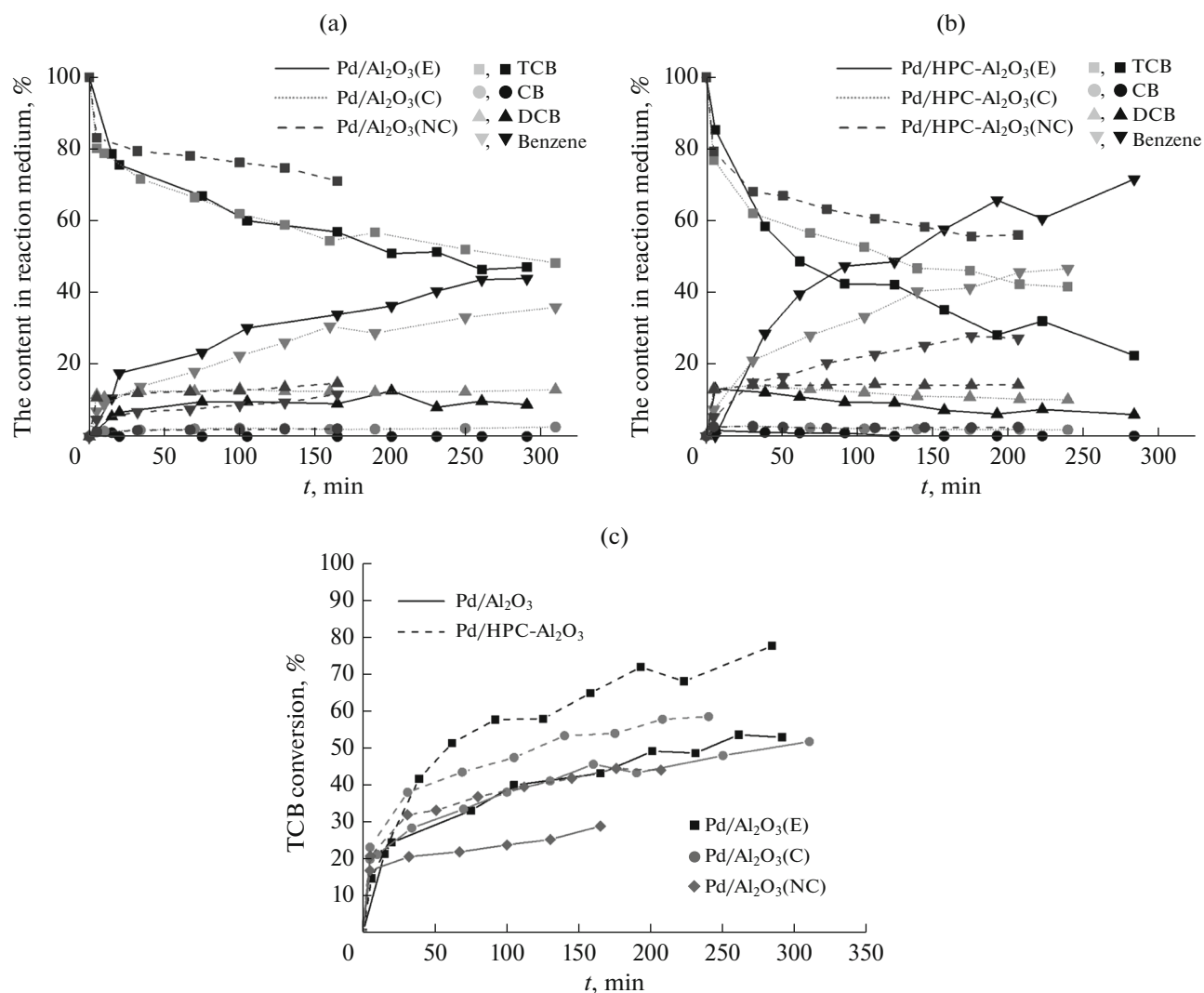


**Fig. 1.** Kinetic curves of 1,3,5-trichlorobenzene hydrodechlorination in the presence of (a) nonmodified catalyst samples and (b) samples modified by the heteropoly compound; (c) the time dependence of the 1,3,5-trichlorobenzene conversion.

compared to nonmodified  $\text{Pd}/\text{Al}_2\text{O}_3(\text{C})$  and  $\text{Pd}/\text{Al}_2\text{O}_3(\text{E})$  samples.

The observed shape of kinetic curves can be caused by two main reasons: (1) the quasi-steady state of the system, when intermediate products quickly undergo further transformation and, therefore, do not accumulate in the reaction mixture; (2) strong adsorption of intermediates, when they are almost not desorbed from the catalyst surface until benzene forms. Given that  $\text{Al}_2\text{O}_3$  is a good adsorbent, it is more likely that the second option is realized. Thus, it can be assumed that a strong adsorption of 1,3,5-trichlorobenzene occurs on the surface of both types of catalysts, both nonmodified and those with the heteropoly compound; the conversion of 1,3,5-trichlorobenzene to benzene occurs mainly without desorption of intermediates. This is supported by the fact that the content of intermediate compounds in the reaction mixture is almost

the same for catalysts based on different types of  $\text{Al}_2\text{O}_3$ .

Figure 1c shows the time dependences of the conversion of 1,3,5-trichlorobenzene in the reaction mixture for all samples. Each kinetic curve has two characteristic segments. In the initial period (the first 10 min of an experiment) the reaction rate on all catalysts is high. Then, under the action of the reaction medium, it noticeably decreases, apparently as a result of the partial deactivation of the active sites of the catalyst. The duration of the first period is approximately the same for all nonmodified catalysts (Fig. 1c), which indirectly may indicate a similar nature of their deactivation. The experimental points of the second segment of the kinetic curve are well described by a linear relationship ( $R^2 > 0.9$ , where  $R$  is the correlation coefficient). That is, the reaction order in this segment is close to zero, which is very likely when all active sur-

**Table 1.** Designations and properties of catalysts. The values of catalytic activity are given for the 1st (initial) and 2nd segments of the kinetic curve

Sample	Type of Al <sub>2</sub> O <sub>3</sub>	HPC content, wt %	S <sub>BET</sub> , m <sup>2</sup> /g	d <sub>pore</sub> , nm	t <sub>50</sub> <sup>a</sup> , min	t <sub>30</sub> <sup>b</sup> , min	TOF, h <sup>-1</sup>	
							1st segment	2nd segment
Pd/Al <sub>2</sub> O <sub>3</sub> (E)	Engelhard	—*	173 ± 17	4.1	180	0	11 <sup>c</sup>	0.6
Pd/Al <sub>2</sub> O <sub>3</sub> (C)	Calcined at 600°C	—*	263 ± 26	5.5	250	4	30	0.7
Pd/Al <sub>2</sub> O <sub>3</sub> (NC)	Not calcined	—*	220 ± 22	—**	—***	65	25.6	0.3
Pd/HPC–Al <sub>2</sub> O <sub>3</sub> (E)	Engelhard	20	177 ± 18	4.1	62	5	18.2	0.9
Pd/HPC–Al <sub>2</sub> O <sub>3</sub> (C)	Calcined at 600°C	20	241 ± 24	6.7	105	8	34.6	0.7
Pd/HPC–Al <sub>2</sub> O <sub>3</sub> (NC)	Not calcined	20	215 ± 21	—**	176	1	31	0.6

The content of palladium in all catalysts was 2 wt %.

<sup>a</sup> Conversion half-time of 1,3,5-trichlorobenzene.

<sup>b</sup> Time for 30% 1,3,5-trichlorobenzene conversion.

<sup>c</sup> The value may be underestimated due to the fact that the first analysis was carried out 15 min after the start of the reaction, and not after 5 min, as in the case of Pd/Al<sub>2</sub>O<sub>3</sub>(C).

\* The specified component is not present in the samples.

\*\* The pore diameter was not determined for the sample.

\*\*\* On this sample, a 50% conversion of 1,3,5-trichlorobenzene was not achieved.

face sites are covered with a reagent. Due to the complete saturation of the surface, the reaction rate does not depend on the concentration of the reagent. Then the observed constant concentration of intermediates in the reaction mixture seems quite logical: the active sites are not freed until the formation of the final product, benzene.

To compare the activity at the initial and second sections on the kinetic curves, we calculated the catalytic activity (turnover frequency, **TOF**) at both segments using the following formula:

$$\text{TOF} = \frac{\Delta C_{\text{TCB}}}{\Delta t n}$$

where  $\Delta C_{\text{TCB}}$  is a change in the concentration of 1,3,5-trichlorobenzene in the reaction mixture for time period  $\Delta t$ , and  $n$  is the content of palladium in the catalyst sample in the reactor ( $2.8 \times 10^{-5}$  mol). Table 1 shows the results obtained.

It is seen that the initial activity of Pd/Al<sub>2</sub>O<sub>3</sub>(E) is somewhat lower than that of Pd/Al<sub>2</sub>O<sub>3</sub>(C) and Pd/Al<sub>2</sub>O<sub>3</sub>(NC), which is due to the delay in taking the first sample for analysis. In the second segments of kinetic curves, the activity of catalysts drops abruptly and becomes comparable for all the three systems, although the deactivating effect of the reaction medium most strongly affects the Pd/Al<sub>2</sub>O<sub>3</sub>(NC) catalyst: its activity decreases from 25.6 to 0.3 h<sup>-1</sup>. The latter value is about two times lower than for the other two nonmodified samples in the corresponding segments of kinetic curves.

Modification by heteropoly compound causes three effects (Fig. 1c): an increase in the initial activity of catalysts on all supports, a significant increase (up

to 100 min) in the duration of the initial period, and a slight increase in activity in the second segments of kinetic curves, especially noticeable for Pd/HPC–Al<sub>2</sub>O<sub>3</sub>(NC).

Pd/HPC–Al<sub>2</sub>O<sub>3</sub>(E) is more stable in the reaction medium than Pd/Al<sub>2</sub>O<sub>3</sub>(E), which can be seen from a slightly higher activity in the second segment of kinetic curves. The activity of the modified and nonmodified catalysts on the Al<sub>2</sub>O<sub>3</sub>(C) support in the second segment of the kinetic curves is the same, and the difference in conversion over comparable periods of reaction is due to the high activity of Pd/HPC–Al<sub>2</sub>O<sub>3</sub>(C) in the initial period of the reaction.

Thus, the catalysts can be arranged in the following order according to the efficiency in 1,3,5-trichlorobenzene hydrodechlorination: Pd/HPC–Al<sub>2</sub>O<sub>3</sub>(E) > Pd/HPC–Al<sub>2</sub>O<sub>3</sub>(C) > Pd/HPC–Al<sub>2</sub>O<sub>3</sub>(NC) ≈ Pd/Al<sub>2</sub>O<sub>3</sub>(E) ≈ Pd/Al<sub>2</sub>O<sub>3</sub>(C) > Pd/Al<sub>2</sub>O<sub>3</sub>(NC). All the studied catalysts lose their activity under the action of the reaction medium, although the deactivation of modified samples is noticeably slower, and the catalyst on the HPC–Al<sub>2</sub>O<sub>3</sub>(E) support is the most resistant to it.

Due to the relatively low efficiency of the Pd/Al<sub>2</sub>O<sub>3</sub>(NC) sample and considering that, during high temperature treatments in the course of the deposition of a heteropoly compound, boehmite should be converted to alumina, which makes this support analogous to Al<sub>2</sub>O<sub>3</sub>(C), the physicochemical properties of the catalysts prepared using Al<sub>2</sub>O<sub>3</sub>(NC) were studied in less detail compared to other samples.

### *Study of the Texture and Morphology of the Sample Surfaces*

The texture and morphology of the samples surface were studied by low-temperature adsorption–desorption of nitrogen and SEM–EDA. Table 1 presents the values of the specific surface area. It is seen that  $S_{\text{BET}}$  and  $d_{\text{pore}}$  of the Pd/Al<sub>2</sub>O<sub>3</sub>(C) catalyst is noticeably higher than in the case of Pd/Al<sub>2</sub>O<sub>3</sub>(E), and the values for Pd/Al<sub>2</sub>O<sub>3</sub>(NC) are in between. Supporting of the heteropoly compound does not lead to a significant change in  $S_{\text{BET}}$ . Analysis of the pore size distribution curves showed that the introduction of a heteropoly compound leads to a decrease in the number of small pores: thus, pores smaller than 4 nm in size becomes noticeably less frequent in the Pd/HPC–Al<sub>2</sub>O<sub>3</sub>(E) catalyst, and disappear in the Pd/HPC–Al<sub>2</sub>O<sub>3</sub>(C) sample. The average pore size does not change after modification in the case of Al<sub>2</sub>O<sub>3</sub>(E), and it slightly increases from 5.5 to 6.7 nm for Al<sub>2</sub>O<sub>3</sub>(C). Thus, the modification of both types of alumina (E and C), the mouths of small pores are closed by modifier particles.

Comparison of microscopic images obtained by scanning electron microscopy (SEM) (Fig. 2) shows that all nonmodified samples include crystallized particles of irregular shape with smooth edges and with a broad size distribution. The average size of Pd/Al<sub>2</sub>O<sub>3</sub>(E) particles is 25 μm. Pd/Al<sub>2</sub>O<sub>3</sub>(E) and Pd/Al<sub>2</sub>O<sub>3</sub>(C) are characterized by the presence of very small particles on the surface of larger ones. There is a greater amount of the small phase of this sort in Pd/Al<sub>2</sub>O<sub>3</sub>(E), and it is almost absent from Pd/Al<sub>2</sub>O<sub>3</sub>(NC). Unlike the other two, this catalyst consists by larger (on average 80 μm) and better crystallized particles, and the distribution of palladium over the surface is less uniform in it than in other samples according to EDA.

Modification by the heteropoly compound leads to significant changes in the morphology of the particles: they become more rounded and have a loose surface. This is likely due to the presence of modifying heteropoly compound or its decomposition products formed during heat treatment on the surface of Al<sub>2</sub>O<sub>3</sub>.

Analysis of the distribution maps of the elements obtained by the SEM–EDA method (Fig. 2) shows that both the palladium and the heteropoly compound are evenly distributed over the Al<sub>2</sub>O<sub>3</sub> surface: there are no places where tungsten or silicon concentrates on the maps, or areas that do not contain these elements. Since during the preparation of the modified samples, the heteropoly compound was supported first followed by the palladium salt, it is reasonable to assume that the palladium particles are deposited predominantly on the surface of the heteropoly compound. Therefore, in the heteropoly compound-modified samples, the interaction of palladium with Al<sub>2</sub>O<sub>3</sub> should be significantly weaker than in their nonmodified analogs.

### *XRD and TEM Study*

The diffraction patterns of all samples have strongly broadened peaks, which indicates that the size of coherent scattering region is small. According to XRD data, Pd/Al<sub>2</sub>O<sub>3</sub>(NC) and Pd/HPC–Al<sub>2</sub>O<sub>3</sub>(NC) contain crystalline AlO(OH) (map in PDF 21-1307). Its content in Pd/Al<sub>2</sub>O<sub>3</sub>(NC) is 36 vol%. Crystalline γ-Al<sub>2</sub>O<sub>3</sub> is present in samples obtained on the basis of Al<sub>2</sub>O<sub>3</sub>(C) and Al<sub>2</sub>O<sub>3</sub>(E) (map in PDF 10-425). Its fraction in Pd/Al<sub>2</sub>O<sub>3</sub>(C) is 67 vol%. The rest of the material is in the X-ray amorphous state. The crystal structure of Al<sub>2</sub>O<sub>3</sub> types (C) and (E) does not differ significantly. The size of coherent scattering region calculated by the Scherrer–Selyakov formula from XRD data (about 5 nm) is approximately the same. Modification by the heteropoly compound leads to a decrease in crystallinity and the size of coherent scattering region (4.3–4.5 nm for Pd/HPC–Al<sub>2</sub>O<sub>3</sub>(C) and Pd/HPC–Al<sub>2</sub>O<sub>3</sub>(E); 3 nm for Pd/HPC–Al<sub>2</sub>O<sub>3</sub>(NC)). None of the samples showed the signs of Pd-containing crystalline phases (Pd, PdO, PdH<sub>x</sub>), probably due to the small size of such particles. For the same reason, in the catalysts containing the heteropoly compound, crystalline phases with tungsten or silicon were not detected. Crystalline silica phases were found in a specially prepared sample of the heteropoly compound calcined at 450°C, which points to at least partial decomposition of the heteropoly compound, but tungsten-based crystalline phases (initial heteropoly acid, WO<sub>3</sub>, and HWO<sub>4</sub>) were not identified, probably because they are X-ray amorphous.

Figure 3 shows TEM data for Pd/Al<sub>2</sub>O<sub>3</sub>(C), Pd/Al<sub>2</sub>O<sub>3</sub>(NC), and Pd/Al<sub>2</sub>O<sub>3</sub>(E). It is seen that the morphology of the particles of C, NC, and E supports differs substantially. The Pd/Al<sub>2</sub>O<sub>3</sub>(C) sample (Fig. 3e) contains well-crystallized formations of spherical and columnar shape. The columns have a length up to 50 nm and a thickness up to 5 nm, which is characteristic of γ-Al<sub>2</sub>O<sub>3</sub> obtained by calcination at 500–700°C of boehmite after precipitation from aluminum isopropoxide [25]. The Pd/Al<sub>2</sub>O<sub>3</sub>(NC) image (Fig. 3i) also shows columnar structures, although their content is less and they are shorter shorter on average. In the Pd/Al<sub>2</sub>O<sub>3</sub>(E) sample (Fig. 3a), the shape of the particles of aluminum oxide is round or close to that. The higher crystallinity of Al<sub>2</sub>O<sub>3</sub>(C) compared to Al<sub>2</sub>O<sub>3</sub>(NC) (67 and 36%, respectively) was confirmed by the XRD method.

Figure 3 also shows HRTEM images taken in the bright and dark field modes. The maps of palladium distribution in the sample, and its particle size distribution diagrams are presented as well.

In the dark field mode, bright palladium particles are clearly seen. Its presence has also been confirmed by local EDA in the TEM study. In all samples, palladium particles have nanometer-scale sizes, and no

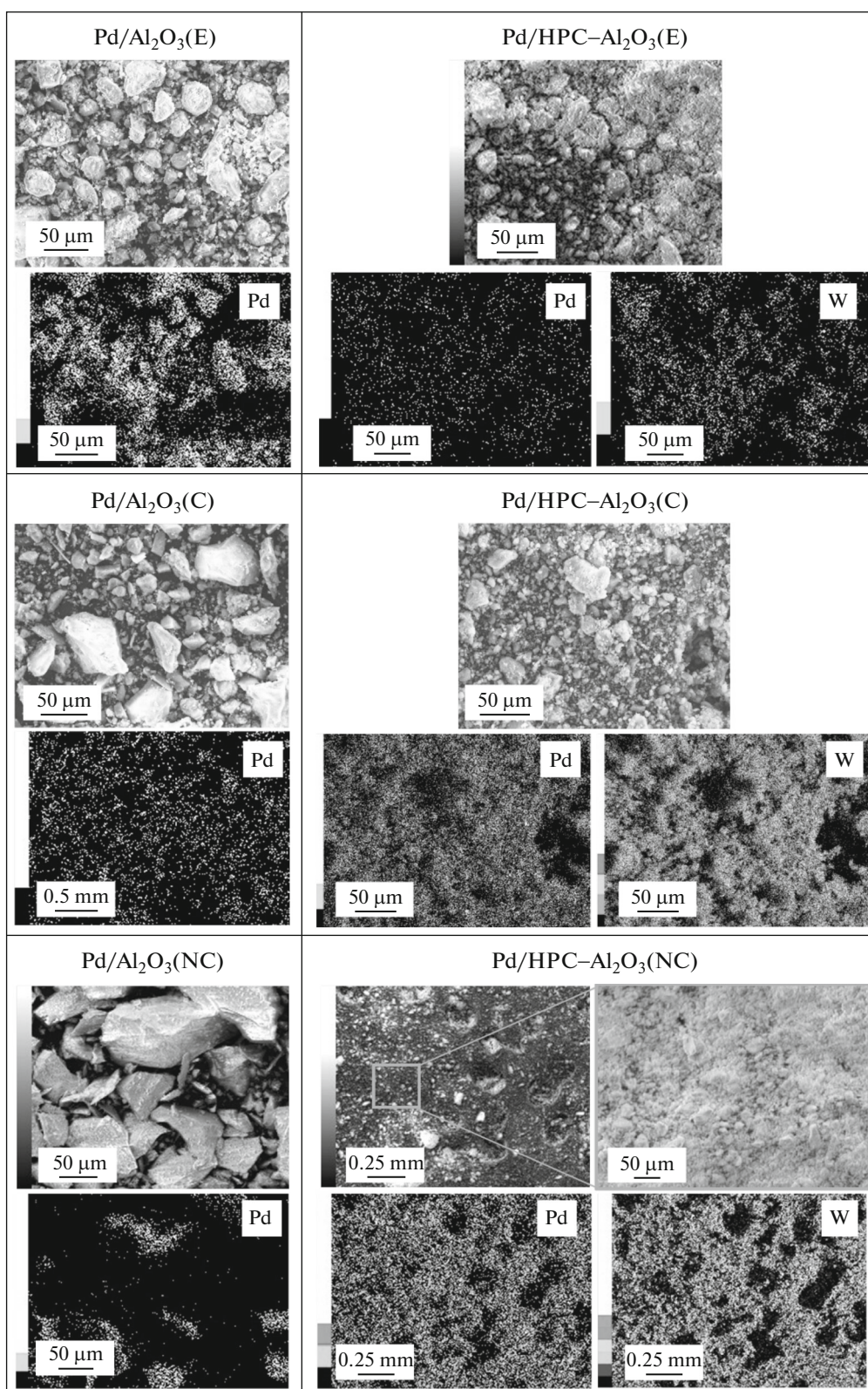
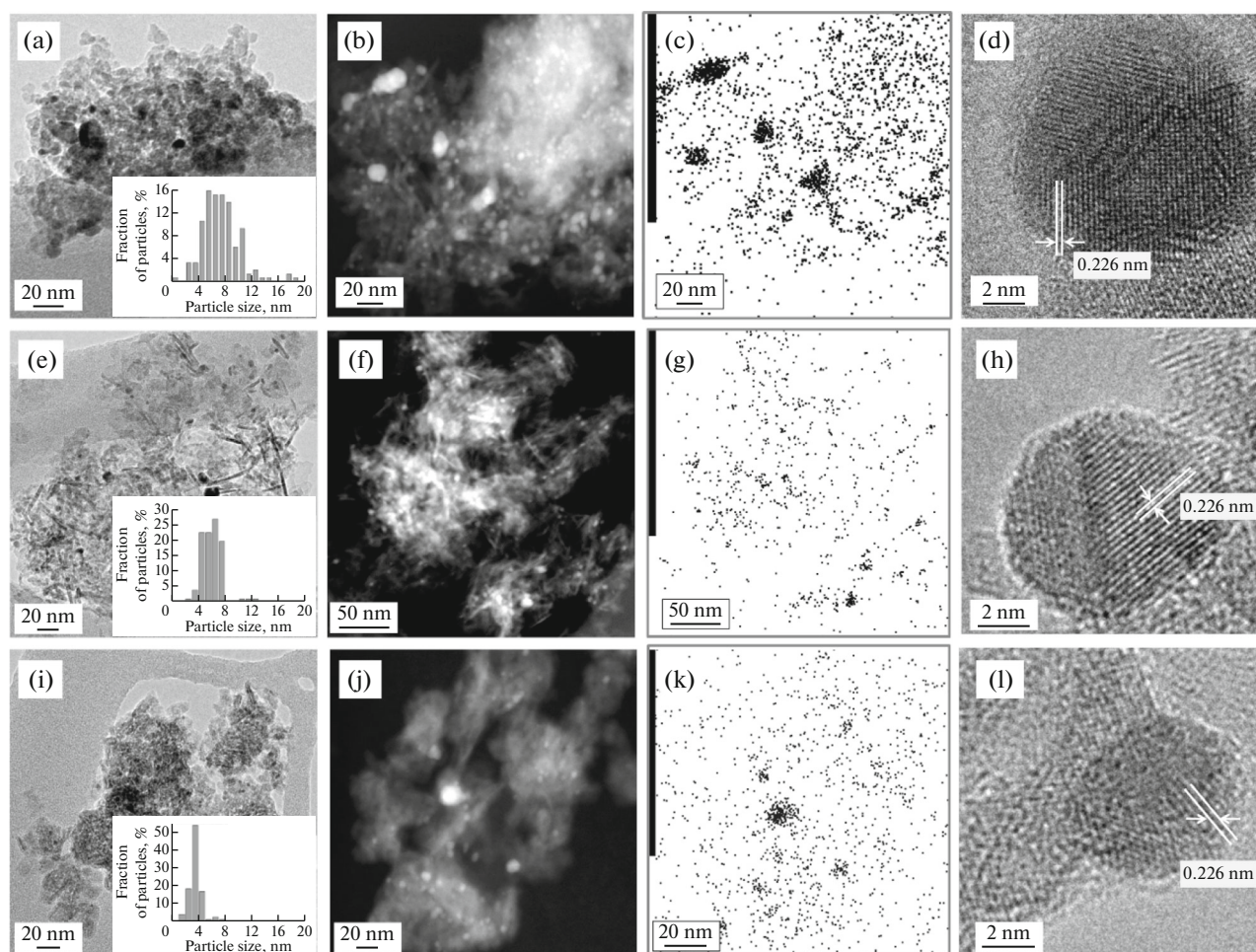


Fig. 2. SEM images of the samples and element distribution maps.



**Fig. 3.** TEM images of the samples in the (a, e, i) bright and (b, f, j) dark field modes; (a, e, i) particle size distribution, (c, g, k) palladium distribution maps Pd, and (d, h, l) HRTEM images: (a–d) Pd/Al<sub>2</sub>O<sub>3</sub>(E), (d–h) Pd/Al<sub>2</sub>O<sub>3</sub>(C), (i–l) Pd/Al<sub>2</sub>O<sub>3</sub>(NC).

particle size >20 nm has been found in any of them. The minimum size and the narrowest Pd particle size distribution are characteristic of Pd/Al<sub>2</sub>O<sub>3</sub>(NC) (Fig. 3l): >50% of particles have a diameter of 4 nm. The Pd/Al<sub>2</sub>O<sub>3</sub>(C) sample contains larger particles, with sizes mainly in the range from 4 to 8 nm. In the Pd/Al<sub>2</sub>O<sub>3</sub>(E) catalyst, the distribution of Pd particles is even wider; most of them have a diameter from 4 to 11 nm, but some are larger. According to HRTEM, all samples contain crystalline palladium particles with a round shape with interplanar spacings of 0.226 nm, characteristic of Pd(111).

Modification by the heteropoly compound leads to a significant change in the structure observed by TEM (Figs. 4 and 5): on the microscopic image of the Pd/HPC–Al<sub>2</sub>O<sub>3</sub>(E) and Pd/HPC–Al<sub>2</sub>O<sub>3</sub>(C) samples, there are small dark areas, uniform in size (approximately 0.5 nm), evenly spaced on the Al<sub>2</sub>O<sub>3</sub> surface. Given their abundance, it can be assumed that they belong to tungsten-containing particles, since the content of the heteropoly compound (20%) is significantly higher than that of palladium (2%). A compar-

ison of microscopic images obtained in the dark field mode and the results of local elemental analysis in various areas (see Figs. 4 and 5) shows that the bright points correspond to palladium particles, while tungsten is distributed over the Al<sub>2</sub>O<sub>3</sub> surface uniformly and its compounds do not form large particles. It is clearly seen in Fig. 5 that palladium and tungsten are simultaneously present in the region of the brightest points, while in the less bright region only tungsten is observed. When supported on modified Al<sub>2</sub>O<sub>3</sub>, palladium is likely localized in the areas covered by the heteropoly compound. Judging from several dark-field images, the particle sizes of palladium range from 2 to 8 nm.

Note that the small diameter of the particles of the heteropoly compound or its decomposition products determined by TEM, did not allow the analysis of the dispersion by XRD.

#### *Study of Catalysts by TPR-H<sub>2</sub>*

Figure 6 shows the TPR-H<sub>2</sub> profiles of precursors of prepared catalysts (before reduction). For all sam-

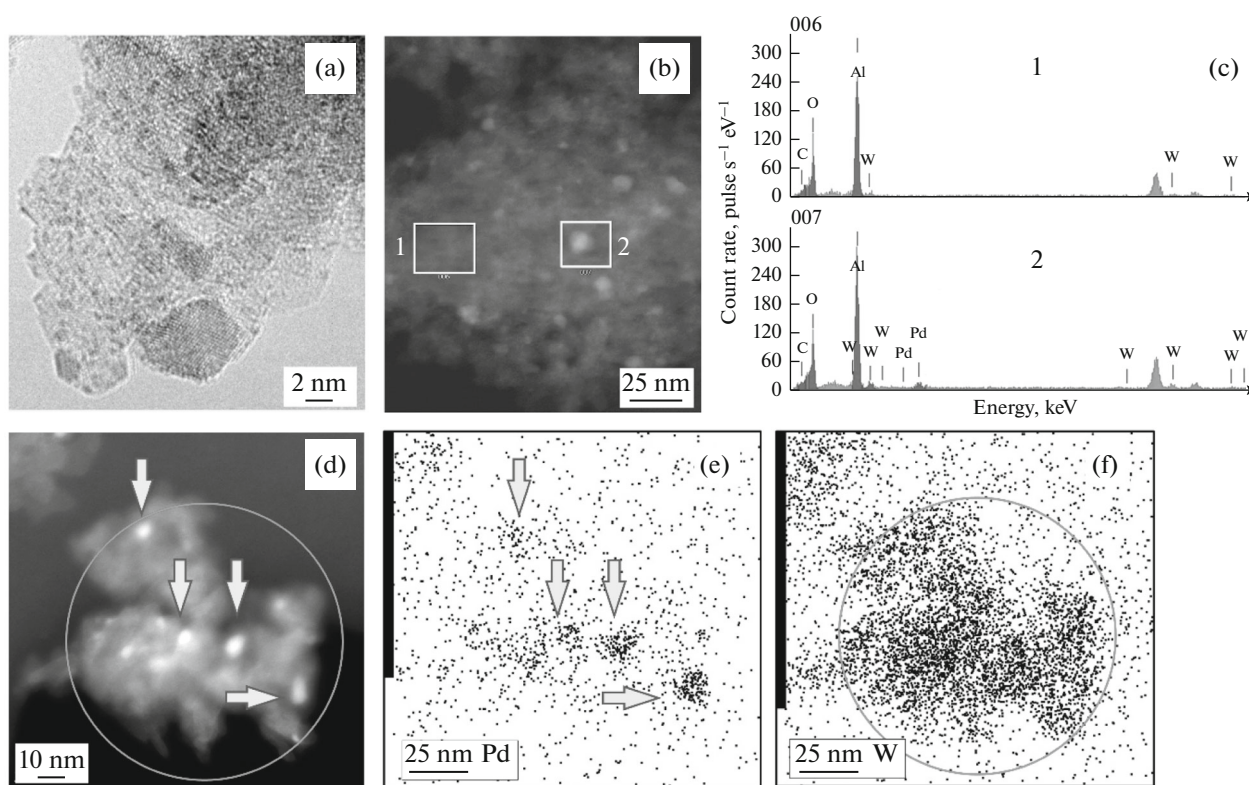


**Fig. 4.** HRTEM images of the Pd/HPC–Al<sub>2</sub>O<sub>3</sub>(E) sample in the (a) bright and (b, d) dark field modes; (c) the results of EDA and (e, f) Pd and W distribution maps.

ples, a negative peak is observed with a maximum at about 76°C, corresponding to the evolution of hydrogen in hydride  $\beta$ -PdH<sub>x</sub> decomposition. Therefore, already during the preliminary purging of the TPR-H<sub>2</sub> setup with hydrogen at 30°C, some of the palladium is reduced from oxide and the Pd<sup>0</sup> particles are saturated with hydrogen to produce  $\beta$ -PdH<sub>x</sub>, which decomposes with evolution of hydrogen during heating after the start of analysis. Atomically dispersed palladium [26] and its small particles are not capable of forming a hydride: according to Boudart [27], the solubility of hydrogen in palladium tends to zero as the dispersion of particles approaches 100%. Not only the ability of at least part of palladium in the catalyst precursor to be easily reduced from oxide already at 30°C, but also the formation of relatively large (in the nanometer range) Pd metal particles during such reduction. The formation of fairly large (in the nanometer range) metal particles during reduction is also pointed to by this fact.

The position of the maximum of the hydrogen evolution peak is the same for all samples except for Pd/Al<sub>2</sub>O<sub>3</sub>(NC) for which it is slightly shifted to the low-temperature region and Pd/HPC–Al<sub>2</sub>O<sub>3</sub>(C) in the TPR-H<sub>2</sub> profile of which the maximum is shifted to higher temperatures. The drift toward high temperatures can be explained by the increased size of PdO particles [28]. The observed difference agrees

with the TEM data, which indicates a smaller palladium particle size in Pd/Al<sub>2</sub>O<sub>3</sub>(NC) compared to Pd/Al<sub>2</sub>O<sub>3</sub>(C).

The TPR-H<sub>2</sub> profiles of all nonmodified samples also contain broad peaks of hydrogen absorption with diffuse maxima at 180, 310, 410, and 530°C, which indicates the presence of PdO particles of different sizes [28, 29] strongly and weakly bound to the surface [28]. Thus, in [29], the hydrogen absorption peaks at  $T = 363$  and 355°C were assigned to the reduction of PdO particles of relatively small size and hydroxyl groups on the surface of alumina. Although Al<sub>2</sub>O<sub>3</sub> that does not contain palladium can only be reduced at  $T > 700^\circ\text{C}$ , hydroxyl groups on its surface are reduced already at temperatures below 400°C in the presence of a catalytically active metal [30].

Large PdO crystallites are first reduced to a metal that is capable of adsorbing and dissociating H<sub>2</sub> molecules. The formed atoms or ions flow onto the surface of Al<sub>2</sub>O<sub>3</sub> and smaller palladium particles by the spillover mechanism and contribute to their reduction at elevated temperatures. The overstoichiometric uptake of hydrogen due to spillover onto the support can also cause hydrogen absorption at  $T > 300^\circ\text{C}$  [28]. Moreover, it is possible that the presence of high-temperature peaks is due to the reduction of atomically dispersed palladium.

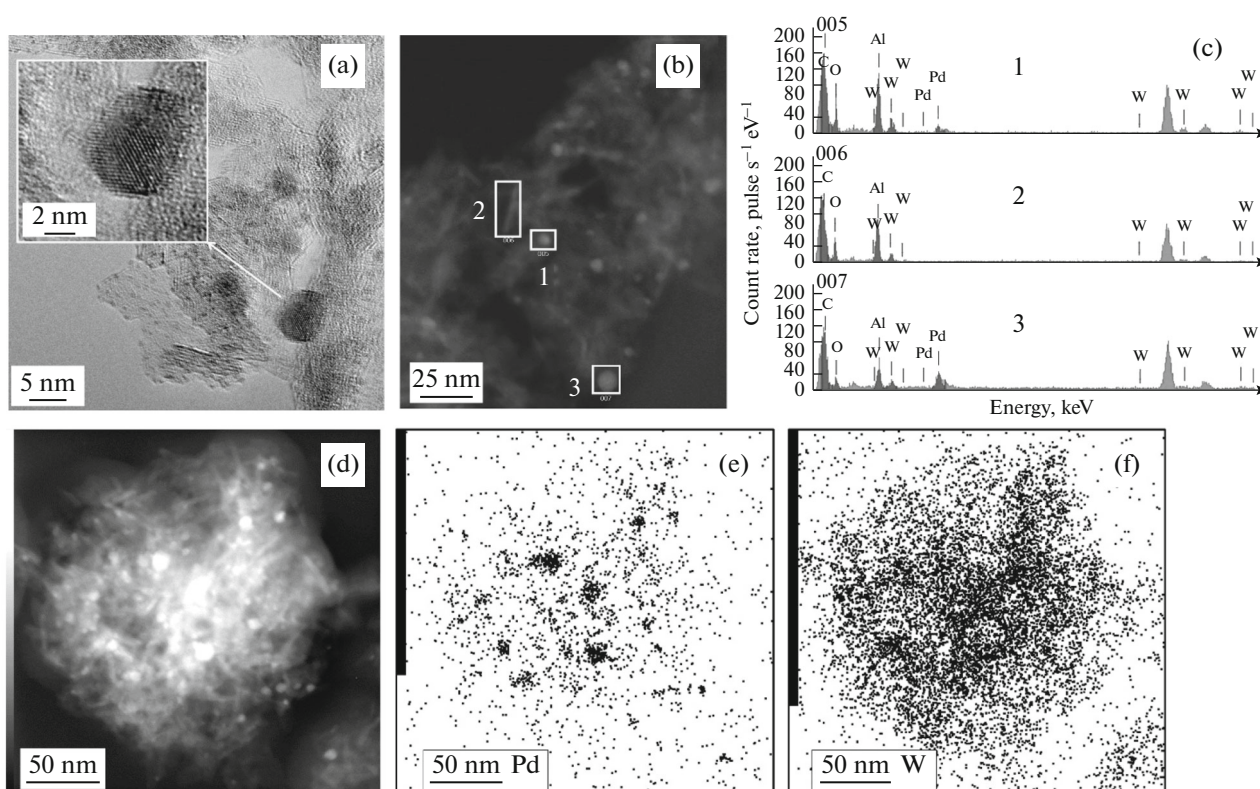
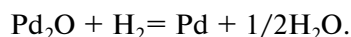


**Fig. 5.** HRTEM images of the Pd/HPC–Al<sub>2</sub>O<sub>3</sub>(C) sample in the (a) bright and (b, d) dark field modes; (c) the results of EDA and (e, f) Pd and W distribution maps.

The peak at 180°C seems to be associated with the partial reduction of PdO to Pd<sub>2</sub>O [20]:



whereas the second stage of reduction occurs at higher temperatures and corresponds to a peak with a maximum at 530°C:



The peak intensity at 180°C is at maximum for the Pd/Al<sub>2</sub>O<sub>3</sub>(NC) sample, lower for Pd/Al<sub>2</sub>O<sub>3</sub>(C) and minimal for Pd/Al<sub>2</sub>O<sub>3</sub>(E). The latter sample is characterized by the largest peak area at 530°C (data on hydrogen absorption are given in Table 2). It can be assumed that, in the composition of the Pd/Al<sub>2</sub>O<sub>3</sub>(E) precursor, the main part of PdO is strongly bound with the support.

Based on the results of TPR-H<sub>2</sub>, palladium reduction temperature was chosen to be 500°C, since isothermal reduction of almost all forms of palladium present in the precursors is possible at this temperature.

After the modification of catalysts on Al<sub>2</sub>O<sub>3</sub>(C) and Al<sub>2</sub>O<sub>3</sub>(NC) supports by the heteropoly compound, the intensity of hydrogen absorption peaks at 180–530°C noticeably decreases (Table 2), and remains almost unchanged in the case of Pd/HPC–Al<sub>2</sub>O<sub>3</sub>(E), but all the peaks shift towards lower temperatures. The

observed changes can be attributed to the weakening of the interaction of PdO with the Al<sub>2</sub>O<sub>3</sub> surface. As a result, most of the PdO is reduced at relatively low temperatures. Indeed, the area of the low-temperature peak of hydrogen evolution corresponding to the decomposition of palladium hydride in Pd/HPC–Al<sub>2</sub>O<sub>3</sub>(NC) and Pd/HPC–Al<sub>2</sub>O<sub>3</sub>(C) sample profiles increases (Table 2), but such a growth is not observed for Pd/HPC–Al<sub>2</sub>O<sub>3</sub>(E). The obtained data suggest that a peak at  $T = 500\text{--}530^\circ\text{C}$  characterizes the reduction of PdO in the form of well-structured relatively large particles and/or particles strongly bound to the Al<sub>2</sub>O<sub>3</sub> surface. This assumption is confirmed by TEM data, according to which the size distribution of palladium particles is the widest for Pd/Al<sub>2</sub>O<sub>3</sub>(E), and the fraction of large particles in it is maximal compared to Pd/Al<sub>2</sub>O<sub>3</sub>(C) and Pd/Al<sub>2</sub>O<sub>3</sub>(NC) samples.

A very strong decrease in the intensity of broad peaks in the temperature range 300–450°C as a result of the modification by heteropoly compound can be explained by a decrease in the degree of interaction of palladium with the Al<sub>2</sub>O<sub>3</sub> surface and by a decrease in the fraction of hydroxyl groups available for reduction on the Al<sub>2</sub>O<sub>3</sub> surface as a result of uniform (according to SEM and TEM) distribution of modifier over the surface.

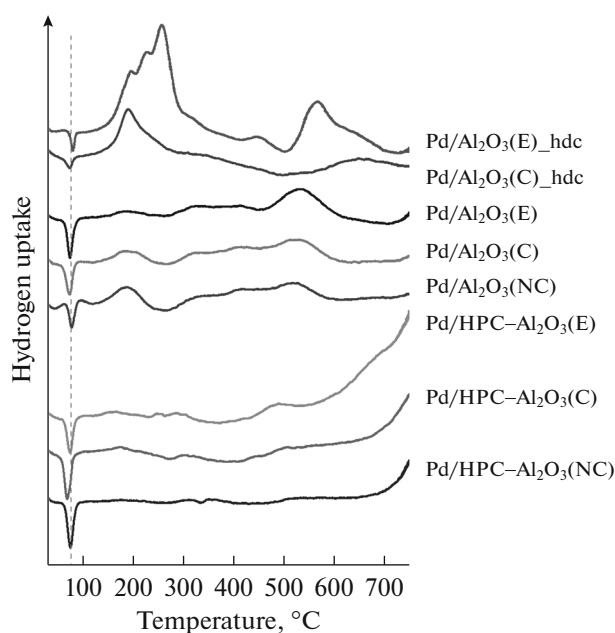


**Fig. 6.** TPR- $H_2$  profiles of nonreduced catalyst precursors and catalysts after tests in hydrodechlorination (denoted as hdc).

An increase in hydrogen uptake at temperatures above  $650^\circ\text{C}$  is caused by the beginning of reduction of the heteropoly compound [31]. In the case of Pd/HPC- $\text{Al}_2\text{O}_3(\text{E})$ , this process begins much earlier, at  $550^\circ\text{C}$ , apparently due to less close contact of the heteropoly compound with the support, which is associated with the morphology of  $\text{Al}_2\text{O}_3(\text{E})$  particles.

Data obtained by the TPR- $H_2$  method confirm the decrease in the degree of interaction of palladium with the support during its modification by heteropoly compound and a change in the composition of the

hydroxyl cover on the  $\text{Al}_2\text{O}_3$  surface and the respective acidic properties of the surface.

#### *Study of Catalysts by Diffuse Reflectance Infrared Fourier Transform Spectroscopy of Adsorbed CO*

Figure 7 shows the DRIFT spectra of adsorbed CO for modified and nonmodified samples of  $\text{Al}_2\text{O}_3(\text{E})$  and  $\text{Al}_2\text{O}_3(\text{C})$ . Absorption at  $2250\text{--}2150\text{ cm}^{-1}$  is due to CO complexes with aluminum cations on the support surface.

The spectrum of the initial  $\text{Al}_2\text{O}_3$  samples contains an absorption band with a maximum at  $2200\text{ cm}^{-1}$ , which refers to CO complexes with coordination-unsaturated  $\text{Al}^{3+}$  cations in tetrahedral coordination on the segments of the surface with an ordered structure: Lewis acid sites (LASs) of the  $L_3$  type according to Morterra's classification [32–34]. The intensity of this absorption band increases with increasing CO pressure from 5 to 55 Torr, which is associated with the filling of free LAS- $L_3$  sites. Also, for both types of  $\text{Al}_2\text{O}_3$ , the spectrum has a shoulder in the region of  $2216\text{--}2219\text{ cm}^{-1}$ , which can correspond to complexes with LASs of the  $L_2$  type, in which aluminum cations are located near surface defects [32, 33].

The  $\text{Al}_2\text{O}_3(\text{E})$  spectrum additionally comprises an absorption band at  $\sim 2240\text{ cm}^{-1}$ , which is characteristic of carbonyl complexes with LASs of the  $L_1$  type [32, 33]. At a low CO pressure, complexes are predominantly formed with this type of LAS. These sites are covered already at a low pressure of CO, and subsequent pressure increase to 55 Torr does not affect the intensity of this band. With an increase in the CO pressure, LAS- $L_3$  are gradually covered, which can be clearly seen by the intensity of the absorption band at  $2190\text{--}2220\text{ cm}^{-1}$ .

**Table 2.** Hydrogen uptake at different segments of TPR- $H_2$  profiles

Sample	Hydrogen uptake at temperatures, $\mu\text{mol/g}$			
	$76^\circ\text{C}^a$	$190^\circ\text{C}$	$290\text{--}450^\circ\text{C}$	$530^\circ\text{C}$
Pd/ $\text{Al}_2\text{O}_3(\text{E})$	–18	6	27	63
Pd/ $\text{Al}_2\text{O}_3(\text{C})$	–16	26	152	
Pd/ $\text{Al}_2\text{O}_3(\text{NC})$	–10	34	134	
Pd/HPC- $\text{Al}_2\text{O}_3(\text{E})$	–17	5	11	15
Pd/HPC- $\text{Al}_2\text{O}_3(\text{C})$	–23	6	7	8
Pd/HPC- $\text{Al}_2\text{O}_3(\text{NC})$	–21	0	3	4
Pd/ $\text{Al}_2\text{O}_3(\text{E})$ after catalytic test	–5	264 <sup>b</sup>		128
Pd/ $\text{Al}_2\text{O}_3(\text{C})$ after catalytic test	–7	106	–	–

The content of palladium in 1 g of each sample is 0.02 g (188  $\mu\text{mol}$ ).

<sup>a</sup> Negative values correspond to the hydrogen evolution.

<sup>b</sup> Hydrogen absorption in the temperature range  $145\text{--}326^\circ\text{C}$ .

Dashes mean that in these areas there are no peaks in TPR profiles.

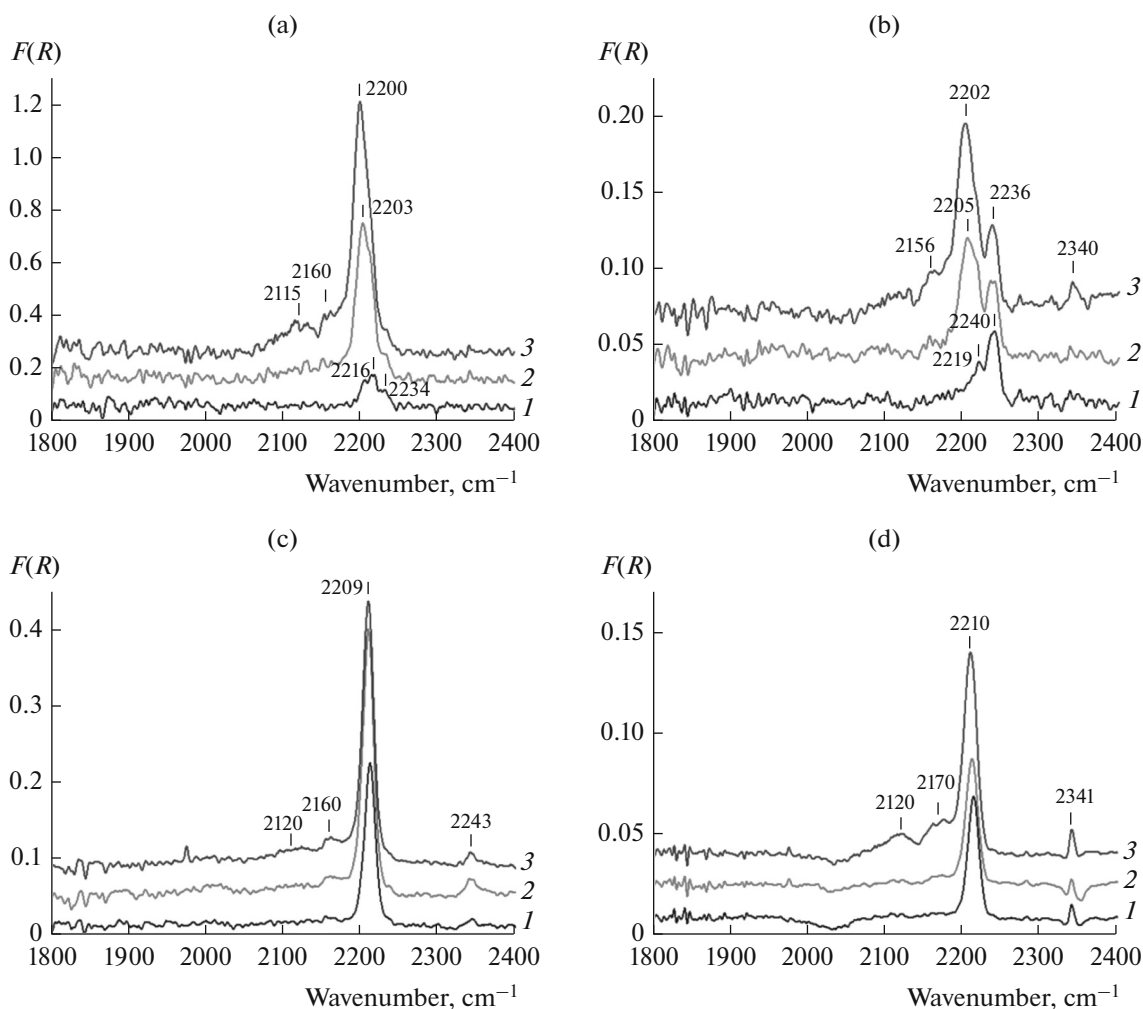


**Fig. 7.** DRIFT spectra of CO adsorbed on alumina (a)  $\text{Al}_2\text{O}_3(\text{C})$  and (b)  $\text{Al}_2\text{O}_3(\text{E})$  and alumina modified by the heteropoly compound (c)  $\text{HPC-Al}_2\text{O}_3(\text{C})$  and (d)  $\text{HPC-Al}_2\text{O}_3(\text{E})$ . CO pressure: 5 (curves 1), 20 (curves 2), and 50 Torr (curves 3).<sup>1</sup>

The appearance of IR spectrum in the range 2250–2150  $\text{cm}^{-1}$  for modified samples changes. After the deposition of the heteropoly compound, the absorption bands at 2235–2240 and 2002–2205  $\text{cm}^{-1}$  disappear, and the intensity of the absorption band at 2209–2215  $\text{cm}^{-1}$  increases. It is likely that the heteropoly compound blocks most of the LASs of the ordered surface and fills their coordination sphere, which leads to the weakening or complete disappearance of LAS- $L_1$  and LAS- $L_3$ . The number of LAS- $L_2$ , on the contrary, increases. It is possible that the modification by the heteropoly compound contributes to the transition of a part of aluminum cations to a new coordination state, which coincides in coordination number with  $L_2$ -type sites. With the influence of the new coordination sphere, the electron-accepting capacity of the sites increases. An alternative explanation is the formation of LASs of a new nature upon the deposition of the heteropoly compound. The formation of additional LASs as a result of the adsorption of

tungsten oxides on the  $\text{Al}_2\text{O}_3$  surface was reported in [35–37].

The electronic state of palladium particles on the surface of catalysts was studied by the same method by tracking the change of the absorption bands of adsorbed CO (Fig. 8). In the  $\text{Pd}/\text{Al}_2\text{O}_3(\text{E})$  spectrum (Fig. 8a), absorption bands characteristic of CO adsorption on  $\text{Pd}^0$  are observed. The absorption band at 2091–2095  $\text{cm}^{-1}$  corresponds to linear  $\text{Pd}^0\text{-CO}$  complexes. The absorption band at 1990  $\text{cm}^{-1}$  with a shoulder at 1950  $\text{cm}^{-1}$  can be attributed to bridging complexes of CO with two adjacent palladium atoms  $\text{Pd}^0\text{-CO}$ . The absorption at 1800–1900  $\text{cm}^{-1}$  indicates the contribution of the CO bridging complexes coordinated by three palladium atoms  $(\text{Pd}^0)_3\text{-CO}$  [38–41].

The intensity of the absorption band corresponding to the linear complex is approximately three times lower than for the bridge complexes. According to the literature data, this intensity ratio is characteristic of

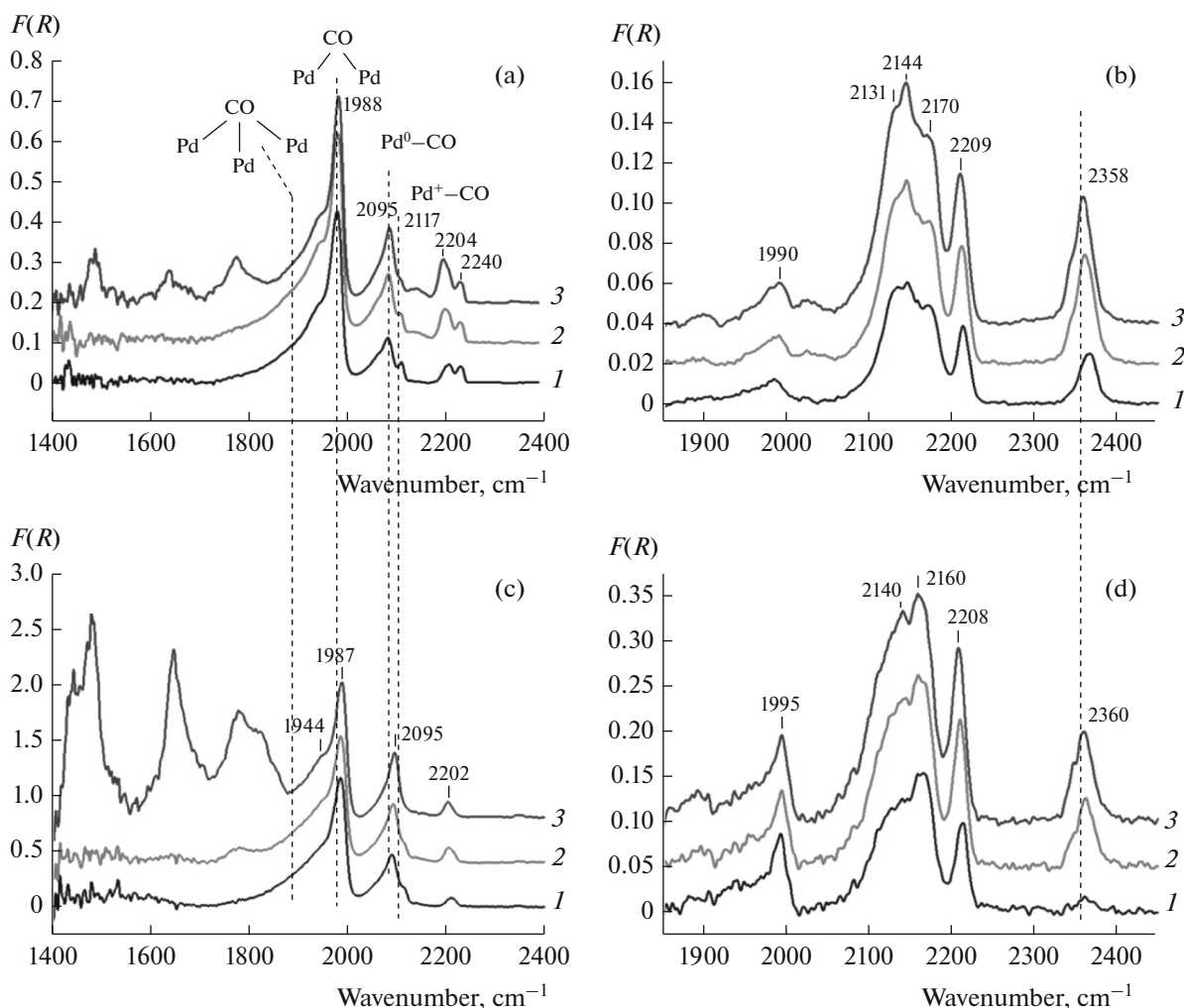


**Fig. 8.** DRIFT spectra of CO adsorbed on the surface of (a) Pd/Al<sub>2</sub>O<sub>3</sub>(E), (b) Pd/Al<sub>2</sub>O<sub>3</sub>(C), (c) Pd/HPC–Al<sub>2</sub>O<sub>3</sub>(E) and (d) Pd/HPC–Al<sub>2</sub>O<sub>3</sub>(C). CO pressure: 5 (curves 1), 20 (curves 2), and 50 Torr (curves 3).

molecules occupying two sites in the unit cell [39], which is consistent with the TEM detection of crystallized palladium particles. In the case of palladium atomically dispersed on the surface (particles are smaller than 2 nm), the spectrum contains an intense band in the range 2070–2110 cm<sup>-1</sup> corresponding to linear complexes [42, 43]. The broad absorption band of bridging complexes with a blurred shoulder in the region of smaller wavenumbers indicates the adsorption of CO molecules on different faces of palladium particles.

The absorption band at 2120–2117 cm<sup>-1</sup> can be attributed to linear CO complexes with oxidized palladium Pd<sup>+</sup>–CO [44]. Binet et al. [38] note that absorption at 2100–2150 cm<sup>-1</sup> is characteristic of CO complexes with partially oxidized palladium, and the absorption bands corresponding to (Pd<sup>2+</sup>)–CO complexes lie in the range of higher wavenumbers (2215–2145 cm<sup>-1</sup>). The absorption band of Pd<sup>+</sup>–CO is read-

ily seen in the spectrum obtained at a low CO pressure. Apparently, these sites are one of the first to be filled with adsorbed CO molecules.

As the CO pressure increases from 5 to 55 Torr, the absorption band corresponding to the linear complex Pd<sup>0</sup>–CO shifts from 2070 to 2095 cm<sup>-1</sup>. Bertarione et al. [40] associate the absorption band at 2070 cm<sup>-1</sup> with linear CO complexes with palladium atoms located on the edges, steps, and terraces of the (100) and (111) faces. Thus, at low pressures of CO, the most defective parts of the surface of palladium are covered. Further adsorption of CO is manifested in the IR spectrum in a slight shift of the corresponding absorption band. The large halfwidth of the absorption band at 2070–2095 cm<sup>-1</sup> [40] and a small shoulder near 2050 cm<sup>-1</sup> [41] indicating the presence of sites of at least two types, point to the inhomogeneity of the palladium surface.

At a CO pressure of 55 Torr, in the 1700–1200  $\text{cm}^{-1}$  region of the Pd/Al<sub>2</sub>O<sub>3</sub>(E) IR spectrum, there are absorption bands associated with the carbonate structures on the Al<sub>2</sub>O<sub>3</sub> surface. Carbonates are formed during the interaction of CO molecules with OH groups on the Al<sub>2</sub>O<sub>3</sub> surface [45, 46].

Unlike Pd/Al<sub>2</sub>O<sub>3</sub>(E), in the DRIFT spectrum of CO adsorbed on Pd/Al<sub>2</sub>O<sub>3</sub>(C) (Fig. 8), the absorption band corresponding to the (Pd<sup>+</sup>)–CO complex is practically absent; that is, almost all palladium is metallic. Moreover, the absorption band characteristic of the (Pd<sup>0</sup>)<sub>3</sub>–CO complexes is not so pronounced. This may be due to the smaller particle size in the specified sample, which is confirmed by the TEM method. At a pressure of 55 Torr, a significantly greater contribution of carbonate structures is also observed compared to the Pd/Al<sub>2</sub>O<sub>3</sub>(E) spectrum.

Thus, Pd<sup>0</sup> is present on the surface of nonmodified catalysts after thermal vacuum treatment; a noticeable contribution of partially oxidized palladium is also characteristic of the Pd/Al<sub>2</sub>O<sub>3</sub>(E) sample. The data obtained by IR spectroscopy are consistent with the TEM findings on the size distribution of Pd particles.

The modification of supports by the heteropoly compound leads to a significant change in the form of the IR spectra of CO adsorbed on palladium catalysts (Figs. 8c, 8d). Thus, the spectra of both Pd/HPC–Al<sub>2</sub>O<sub>3</sub>(C) and Pd/HPC–Al<sub>2</sub>O<sub>3</sub>(E) systems have an absorption band at 2360  $\text{cm}^{-1}$ , which occurs in the presence of CO<sub>2</sub> molecules coordinated on the Al<sub>2</sub>O<sub>3</sub> surface without carbonate formation. The literature does not contain a definitive answer to the question regarding the sites on which adsorption takes place, however, we can assume that they include palladium cations. We attribute the observed absorption bands at 2340  $\text{cm}^{-1}$  and 2365–2358  $\text{cm}^{-1}$  to CO<sub>2</sub> complexes with metallic palladium (Pd<sup>0</sup>...CO<sub>2</sub>) [47].

The superposition of bands in the range 2180–2050  $\text{cm}^{-1}$  may be due to the presence of the absorption band at 2170–2172  $\text{cm}^{-1}$ , which is characteristic of carbonyl complexes Pd<sup>2+</sup>–CO, and absorption bands at 2144 and 2134–2131  $\text{cm}^{-1}$ , which correspond to carbonyl complexes Pd<sup>+</sup>–CO. Apparently, the absorption band at 2157  $\text{cm}^{-1}$  refers to the Pd<sup>2+</sup>–CO complexes. There is also a low-intensity absorption band at 1984–1990  $\text{cm}^{-1}$ , characteristic of complexes with two atoms (Pd<sup>0</sup>)<sub>2</sub>–CO. Thus, unlike samples that do not contain the heteropoly compound, in modified samples, the main form of palladium on the surface is Pd<sup>2+</sup> (less) and Pd<sup>+</sup> (more) cations. There is not so much of metallic palladium, and it is presented both as a metallic phase (the main form in the samples without the heteropoly compound) and individual atoms.

The absorption band at 1900  $\text{cm}^{-1}$  corresponds to bridging CO adsorption, but not on metallic palla-

dium. It is possible that CO is coordinated on the neighboring cations of palladium and aluminum.

The differences of Pd/HPC–Al<sub>2</sub>O<sub>3</sub>(C) spectrum from Pd/HPC–Al<sub>2</sub>O<sub>3</sub>(E) are as follows. In the range 2180–2050  $\text{cm}^{-1}$ , the Pd/HPC–Al<sub>2</sub>O<sub>3</sub>(C) spectrum is dominated by the absorption band at 2164–2159  $\text{cm}^{-1}$ ; that is, there are more Pd<sup>2+</sup>–CO than Pd<sup>+</sup>–CO complexes. The contribution of another absorption band at 2100–2111  $\text{cm}^{-1}$  (manifested as an inflection, but in the spectrum of the Pd/HPC–Al<sub>2</sub>O<sub>3</sub>(E) sample does not even bend) is noticeable, which can be attributed to complexes with single atoms, Pd<sup>0</sup>–CO. There are also a band at 1995  $\text{cm}^{-1}$  of carbonyl complexes (Pd<sup>0</sup>)<sub>2</sub>–CO and the absorption band of the bridge form at 1890  $\text{cm}^{-1}$ .

Thus, the results of IR study demonstrate significant differences in the composition of LASs on the surface of Al<sub>2</sub>O<sub>3</sub>(E) and Al<sub>2</sub>O<sub>3</sub>(C) supports, which leads to different types of palladium coordination during deposition and its different electronic state in the prepared catalysts. All this should affect the catalytic properties of the systems obtained.

There are also significant changes in the organization of the surface as a result of modification by the heteropoly compound. After thermal vacuum treatment, on the surface of catalysts obtained without a heteropoly compound, Pd<sup>0</sup> is the main form, mostly as paired adsorption sites, i.e. relatively large particles. On the contrary, on the surface of catalysts modified by the heteropoly compound, there are mainly single (for CO adsorption) Pd<sup>+</sup> and Pd<sup>2+</sup> cations. Pd<sup>0</sup> adsorption sites are also available, but they are not dominant.

For the Pd/HPC–Al<sub>2</sub>O<sub>3</sub>(E) sample, suppression of the strongest LASs of the support surface was observed, which were present in significant amounts in Al<sub>2</sub>O<sub>3</sub>(E) and absent from Al<sub>2</sub>O<sub>3</sub>(C).

On the surface of the modified catalysts, the appearance of CO<sub>2</sub> is observed, which is coordinated by the surface and formed as a result of CO oxidation, but surface carbonates are not detected in quantities sufficient for reliable registration. On the contrary, on the surface of nonmodified catalysts, a large amount of monodentate, bidentate, and “organic” carbonates are formed as a result of CO oxidation by the surface. This indicates the polymodality of the distribution of the main properties of the surface anions (oxygen) and the presence of surface sites that are active in CO oxidation.

### Discussion

It has been noted in the literature [48] that the structural sensitivity of the hydrodechlorination reaction may be due to the increased resistance of larger (in the nanometer scale) palladium particles to the effects of HCl, while small particles are easily chlori-

nated in the reaction medium. In the case of noble metals deposited on  $\text{Al}_2\text{O}_3$ , as a result of interaction with the LASs on the support surface, small metal particles become electron-deficient and more readily undergo chlorination by adsorbed chlorine (or HCl). However, the kinetic curves of the 1,3,5-trichlorobenzene conversion on the nonmodified  $\text{Pd}/\text{Al}_2\text{O}_3(\text{E})$  and  $\text{Pd}/\text{Al}_2\text{O}_3(\text{C})$  catalysts do not differ despite significant differences in the dispersity of the active component, the specific surface area, the composition of LASs and surface forms of palladium. Apparently, this is due to the presence of palladium nanoparticles in both samples, which are susceptible to partial oxidation under the action of the components of the reaction medium.

The reason for the deactivation of catalysts in the reaction medium may be palladium oxidation in the reactions with chlorine and chloride ion species formed and in the interaction with support. This oxidation reactions should lead to a change in the TPR- $\text{H}_2$  profiles of the deactivated samples after catalysis. The TPR- $\text{H}_2$  profiles of the  $\text{Pd}/\text{Al}_2\text{O}_3(\text{E})$  and  $\text{Pd}/\text{Al}_2\text{O}_3(\text{C})$  samples after catalytic tests are shown in Fig. 6, and the amounts of absorbed/evolved hydrogen are presented in Table 2.

It can be seen that after catalytic tests, the intensity of the negative peak in the TPR- $\text{H}_2$  profile of both samples decreases by approximately three times. The intensity of the group of peaks in the temperature range from 135 to 335°C significantly increases. These peaks characterize various oxidized forms of palladium, presumably chloride and oxide, weakly and strongly bound to the support surface. The shape and width of the above group of peaks are different for these two samples: in the  $\text{Pd}/\text{Al}_2\text{O}_3(\text{E})$  profile after hydrodechlorination, the reduction peak is in the range from 135 to 450°C and has three poorly separated maxima; in the  $\text{Pd}/\text{Al}_2\text{O}_3(\text{C})$  profile, this group looks like one broad peak with a maximum at 185°C.

Palladium chloride can be formed by the interaction of particles of the active component ( $\text{Pd}^0$ ) with chlorine particles on the surface resulting from the dissociative adsorption of 1,3,5-trichlorobenzene, and its oxide is produced as a result of palladium contact with the  $\text{Al}_2\text{O}_3$  support.

The peak of reduction with a maximum at 530°C, which may correspond to palladium forms tightly bound to the support, shifts to higher temperatures after catalytic tests. This indicates the strengthening of palladium binding with the support, for example, as a result of the formation of a layer on the surface of palladium particles, including palladium oxide and chloride. The peak of reduction at 530°C in the TPR profile of  $\text{Pd}/\text{Al}_2\text{O}_3(\text{C})$  after hydrodechlorination shifts to elevated temperatures much more strongly than in the  $\text{Pd}/\text{Al}_2\text{O}_3(\text{E})$  profile after catalytic test, but it has a lower intensity. As it was already shown when discuss-

ing the TEM results, in the  $\text{Pd}/\text{Al}_2\text{O}_3(\text{E})$  sample, the particle size distribution is much wider than in  $\text{Pd}/\text{Al}_2\text{O}_3(\text{C})$ . The chlorination and oxidation of palladium particles of different sizes can lead to the appearance of forms that are reduced in a wider temperature range.

Note that the catalyst where boehmite was used as a support ( $\text{Pd}/\text{Al}_2\text{O}_3(\text{NC})$ ) is most strongly deactivated in the reaction medium. The obvious reason may be the very small particle size of palladium compared to other catalysts and the narrow size distribution. On the other hand, it is known that boehmite is capable of interacting with the base present in the reaction medium at temperatures of 30°C and above. At  $\text{pH} > 7$ , a tetrahydroxyaluminate ion will be formed [49]:



As a result of this interaction, the destruction of the catalyst surface is possible, leading to an additional decrease in the catalyst activity.

The addition of a base to the reaction medium has long been used to increase the efficiency of hydrodechlorination catalysts, including those supported on  $\text{Al}_2\text{O}_3$ . The efficiency increases as a result of binding of the released hydrogen chloride with the formation of salt [11, 50]. However, in aqueous media at elevated pH, the deactivation of catalytic systems is enhanced: for example, in the hydrodechlorination of 4-chlorophenol, the deactivation rate constant  $\text{Pd}/\text{Al}_2\text{O}_3$  was twice as high as at neutral pH [51].

Chlorobenzenes can be adsorbed and activated on both metals and supports. The probability of the latter option increases when supports with Lewis acidity are used. In this case, hydrogen for the reduction of the substrate adsorbed on LAS is supplied by the spillover mechanism from the metal sites of dissociative adsorption [16]. The activation of chlorobenzenes can also occur on the surface of partially oxidized palladium. It is known that, in liquid-phase hydrodechlorination, catalysts are preferable in which the  $\text{Pd}^0/\text{Pd}^{\delta+}$  ratio is close to 1, which creates good conditions for the activation of both chlorobenzenes and hydrogen [52]. The change in this ratio as a result of deposition of the heteropoly compound on the support surface, as evidenced by the DRIFTS findings, provides an observed increase in the TOF on the initial segments of the kinetic curves (Table 1) but does not prevent deactivation under the action of the reaction medium.

The above consideration allows us to explain the formation of small amounts of intermediates (dichloro- and monochlorobenzenes) in the reaction mixture throughout the catalytic experiment. It can be assumed that the catalyst contains sufficiently strong adsorption sites, for example,  $\text{Pd}^{\delta+}$  and LASs on the support surface. The conversion of 1,3,5-trichlorobenzene into the final product of hydrodechlorination, benzene, occurs without desorption of intermediates. The presence of 1,3-dichlorobenzene and chlo-

robenzene in small amounts in the reaction medium is due to the fact that the adsorption equilibrium is strongly shifted toward the adsorbed form.

Another possible explanation for the form of kinetic curves is the occurrence of the reaction sequentially under the conditions of pseudo-steady-state mode, when intermediate compounds do not accumulate and immediately react with hydrogen. In this case, a low concentration of intermediates throughout the entire reaction cycle is caused by their partial desorption from the surface of the catalyst into the volume of the reaction mixture.

In the course of heat treatment, the decomposition of the modifier  $H_8[Si(W_2O_7)_6]$  can occur with the formation of tungsten and silicon oxides. Tarlani et al. showed [53] that, when supported on  $Al_2O_3$  obtained by the sol-gel method or commercial  $Al_2O_3$ , the thermal stability of the  $H_6P_2W_{18}O_{62}$  heteropoly compound with a Dawson structure significantly increases: before deposition, the decomposition of heteropoly compound occurred already at  $250^\circ C$ , and after deposition, the structure was stable when heated to  $620^\circ C$ . At higher temperatures, it began to transform into the Keggin structure. On the contrary, Pizzio et al. [54] observed the degradation of  $[PW_{12}O_{40}]^{3-}$  anion with the formation of tungsten diphosphate in the course of drying the system supported on  $Al_2O_3$  at  $70^\circ C$ . However, Liu et al. [55] found, that upon calcination of the  $H_4SiW_{12}O_{40}H_2O/Al_2O_3$  system (the same compound was used as a modifier in this work) at  $350^\circ C$ , the anions of Keggin-type structure  $H_4SiW_{12}O_{40}$  were found on the surface; after calcination at  $450^\circ C$ —the phase  $W_3O_{13}$ , and  $>550^\circ C$  and higher temperatures,  $W_3O_{13}$ ; at  $550^\circ C$ , the  $WO_3$  phase and separate  $WO_4$  anions were formed.

In the present work, the calcination of  $Al_2O_3$  after the addition of the heteropoly compound was carried out at  $400^\circ C$ , which guarantees the preservation of the Keggin structure in the support on which palladium was deposited. However, all catalysts were reduced at  $500^\circ C$ ; therefore, the presence of tungsten and silicon oxides cannot be excluded in modified catalysts. Indeed, the XRD analysis of the heteropoly compound  $H_8[Si(W_2O_7)_6] \cdot H_2O$  calcined in air at  $450^\circ C$  showed the presence of crystalline silicon oxides of various nature, but tungsten oxides were not detected by this method, probably due to the amorphous state and small particle size. Silicon oxide on the surface can partially block palladium sites, and tungsten oxides, when interacting with hydrogen, can form tungsten bronzes in the course of reduction, which are known for their hydrogenation activity [56].

Using IR spectroscopy, it has been found that modification of the  $Al_2O_3$  surface by the heteropoly compound leads to weakening or complete disappearance of LASs of the  $L_1$  and  $L_3$  types, with a simultaneous increase in the amount of LASs of the  $L_2$  type,

which may be due to modification by the heteropoly compound or its decomposition products. Changes in the acidity of the  $Al_2O_3$  surface in the presence of tungsten oxides are described in the literature [35–37]. Thus, Liu et al. [36] showed that isolated  $WO_4$  tetrahedral particles provide additional LASs on the surface of modified catalysts. The presence of  $WO_4$  particles on the surface of the  $Pd-WO_x(5\%)/Al_2O_3$  catalyst has an excellent promoting effect in glucose hydrogenolysis. This catalyst had good stability (operating time over 200 h).

Wu et al. [37] found that the increase in the number of LASs is due to the presence of coordination-unsaturated  $W^{m+}$  cations, and Brønsted acid sites arise from partially hydrated tungsten-containing particles, including OH groups, coordinated to sites with  $W=O-$ ,  $W-O-W$  and  $W-O-Al$  bonds in  $WO_x$  clusters. Moreover, it was found that the electronic interaction between the Pt and  $WO_x$  clusters leads to the formation of  $Pt^{\delta+}$  particles, which are the active sites for the oxidation of propane. The activation of the C–H bond occurs at the interface of platinum and tungsten oxide.

A similar promoting effect is likely observed when modifying alumina by the heteropoly compound in the catalysts studied in this work. This assumption is supported by an explicit change in the ratio of different types of LASs after the addition of the heteropoly compound as detected by IR spectroscopy. The close contact of palladium and the deposited heteropoly compound is favorable for the formation of new active sites on the contact line or even bimetallic centers, which exhibit increased efficiency in hydrodechlorination [57]. Note that the shift of the absorption peaks in the TPR- $H_2$  profile of the  $Pd/HPC-Al_2O_3(E)$  catalyst as a result of the modification can be explained by the interaction of Pd with tungsten in the composition of the heteropoly compound or its decomposition products. This catalyst is characterized by greater stability of operation compared to catalysts on other supports. That is, new types of active sites are somewhat more resistant to the effects of the reaction medium during hydrodechlorination.

As can be clearly seen from the TEM and TPR data, the uniform distribution of the heteropoly compound and/or its decomposition products on the support surface (boehmite or  $Al_2O_3$ ) leads to a decrease in the degree of palladium interaction with the support, facilitates the reduction of palladium particles at the temperature of reaction medium, which is favorable for the catalyst stability.

## CONCLUSIONS

In this work, we showed that the support structure affects the catalytic properties of 2%Pd/ $Al_2O_3$  catalysts in the multiphase hydrodechlorination of 1,3,5-

trichlorobenzene. In the Pd/Al<sub>2</sub>O<sub>3</sub>(NC) < Pd/Al<sub>2</sub>O<sub>3</sub>(C) < Pd/Al<sub>2</sub>O<sub>3</sub>(E) series, the dispersion of palladium particles decreases and the width of their size distribution increases in the range below 20 nm. According to the results of diffuse reflectance infrared Fourier transform (DRIFT) spectroscopic study of adsorbed CO, relatively large particles of Pd<sup>0</sup> dominate on the surface of all these samples.

Modification by the heteropoly compound (20 wt % H<sub>8</sub>[Si(W<sub>2</sub>O<sub>7</sub>)<sub>6</sub>] · 6H<sub>2</sub>O) helps reduce the size of palladium particles. The temperature-programmed reduction with hydrogen (TPR-H<sub>2</sub>) showed that all catalysts contain palladium hydride along with oxidized metal forms more strongly bound to the surface, which are reduced at elevated temperatures, and their content decreases after modification by the heteropoly compound and increases after catalytic tests.

According to the DRIFTS data of adsorbed CO, the deposition of the heteropoly compound leads to a change in the type of Lewis acid sites on the Al<sub>2</sub>O<sub>3</sub> surface and the electronic state of palladium. On the surface of modified by the heteropoly compound, LASs of L<sub>1</sub> and L<sub>3</sub> types almost completely disappear, while L<sub>2</sub> sites increase in number. Single cations Pd<sup>+</sup> and Pd<sup>2+</sup> are present in the composition of catalysts modified by the heteropoly compound, while the proportion of Pd<sup>0</sup> is substantially smaller. The Lewis acidity of the catalyst surface determine the possibility of 1,3,5-trichlorobenzene adsorption and activation on the support and the spillover of hydrogen from Pd<sup>0</sup>. The complex study carried out in this work indicates the possibility of the formation of new active sites in the interaction of palladium with the heteropoly compound or its thermal decomposition products (tungsten oxides and WO<sub>4</sub> cations on the surface). These structural features contribute to increasing the stability of catalytic systems modified by the heteropoly compound in the multiphase hydrodechlorination of 1,3,5-trichlorobenzene with the formation of mainly benzene.

## FUNDING

This work was performed on the state assignment "Catalysis and Physical Chemistry of the Surface" AAAA-A16-116092810057-8. The authors acknowledge support from Lomonosov Moscow State University Program of Development.

## REFERENCES

- Perosa, A., Selva, M., and Maschmeyer, T., *Chemosphere*, 2017, vol. 173, p. 535.
- Dai, C., Zhou, Y., Peng, H., Huang, S., Qin, P., Zhang, J., Yang, Y., Luo, L., and Zhang, X., *J. Ind. Eng. Chem.*, 2018, vol. 62, p. 106.
- Zinovyev, S.S., Shinkova, N.A., Perosa, A., and Tundo, P., *Appl. Catal., B*, 2005, vol. 55, p. 39.
- Tundo, P., Perosa, A., Selva, M., and Zinovyev, S.S., *Appl. Catal., B*, 2001, vol. 32, p. L1.
- Cobo, M., Quintero, A., and Correa, C.M.D., *Catal. Today*, 2008, vols. 133–135, p. 509.
- Wu, Y., Gan, L., Zhang, S., Song, H., Lu, C., Li, W., Wang, Z., Jiang, B., and Li, A., *J. Hazard. Mater.*, 2018, vol. 356, p. 17.
- Cheng, L., Jin, Z., and Wang, X., *Catal. Commun.*, 2013, vol. 41, p. 60.
- Han, B., Liu, W., Li, J., Wang, J., Zhao, D., Xu, R., and Lin, Z., *Water Res.*, 2017, vol. 120, p. 199.
- Nieto-Sandoval, J., Munoz, M., de Pedro, Z.M., and Casas, J.A., *Chemosphere*, 2018, vol. 213, p. 141.
- De Corte, S., Sabbe, T., Hennebel, T., Vanhaecke, L., De Gussemme, B., Verstraete, W., and Boon, N., *Water Res.*, 2012, vol. 46, p. 2718.
- Wu, K., Qian, X., Chen, L., Xu, Z., Zheng, S., and Zhu, D., *RSC Adv.*, 2015, vol. 5, p. 18702.
- El-Sharnouby, O., Boparai, H. K., Herrera, J., and O'Carroll, D.M., *Chem. Eng. J.*, 2018, vol. 342, p. 281.
- Mori, T., Kubo, J., and Morikawa, Y., *Appl. Catal., A*, 2004, vol. 271, p. 69.
- Śrębowata, A., Juszczyk, W., Kaszkur, Z., and Karpiński, Z., *Catal. Today*, 2007, vol. 124, p. 28.
- Diaz, E., Mohedano, A.F., Casas, J.A., Shalaby, C., Eser, S., and Rodriguez, J.J., *Appl. Catal., B*, 2016, vol. 186, p. 151.
- Hashimoto, Y., Uemichi, Y., and Ayame, A., *Appl. Catal., A*, 2005, vol. 287, p. 89.
- Ordóñez, S., Sastre, H., and Díez, F.V., *React. Kinet. Catal. Lett.*, 2000, vol. 70, p. 61.
- Lokteva, E.S., Erokhin, A.V., Kachevsky, S.A., Yermakov, A.Y., Uimin, M.A., Mysik, A.A., Golubina, E.V., Zhanavskina, K.L., Turakulova, A.O., and Lunin, V.V., *Stud. Surf. Sci. Catal.*, 2010, vol. 175, p. 289.
- Klokov, S.V., Lokteva, E.S., Golubina, E.V., Chernavskii, P.A., Maslakov, K.I., Egorova, T.B., Chernyak, S.A., Minin, A.S., and Konev, A.S., *Appl. Surf. Sci.*, 2019, vol. 463, p. 395.
- Babu, N.S., Lingaiah, N., Kumar, J.V., and Prasad, P.S.S., *Appl. Catal., A*, 2009, vol. 367, p. 70.
- Golubina, E.V., Lokteva, E.S., Lunin, V.V., Telegina, N.S., Stakheev, A.Y., and Tundo, P., *Appl. Catal., A*, 2006, vol. 302, p. 32.
- Srikanth, C.S., Kumar, V.P., Viswanadham, B., and Chary, K.V.R., *Catal. Commun.*, 2011, vol. 13, p. 69.
- Navalikhina, M.D., Kavalerskaya, N.E., Lokteva, E.S., Peristy, A.A., Golubina, E.V., and Lunin, V.V., *Russ. J. Phys. Chem. A*, 2012, vol. 86, p. 1792.
- Tundo, P., Perosa, A., and Zinovyev, S., *J. Mol. Catal. A: Chem.*, 2003, vols. 204–205, p. 747.
- Mrabet, D., Vu, M.-H., Kaliaguine, S., and Do, T.-O., *J. Colloid Interface Sci.*, 2017, vol. 485, p. 144.
- Sepúlveda, J.H. and Figoli, N.S., *Appl. Surf. Sci.*, 1993, vol. 68, p. 257.
- Boudart, M. and Hwang, H.S., *J. Catal.*, 1975, vol. 39, p. 44.
- Zheng, Q., Farrauto, R., and Deeba, M., *Catalysts*, 2015, vol. 5, p. 1797.

29. Bhogeswararao, S. and Srinivas, D., *J. Catal.*, 2015, vol. 327, p. 65.
30. Hurst, N.W., Gentry, S.J., Jones, A., and McNicol, B.D., *Catal. Rev.*, 1982, vol. 24, p. 233.
31. Jin, H., Yi, X., Sun, X., Qiu, B., Fang, W., Weng, W., and Wan, H., *Fuel*, 2010, vol. 89, p. 1953.
32. Morterra, C. and Magnacca, G., *Catal. Today*, 1996, vol. 27, p. 497.
33. Morterra, C., Bolis, V., and Magnacca, G., *Langmuir*, 1994, vol. 10, p. 1812.
34. Busca, G., Finocchio, E., and Escribano, V.S., *Appl. Catal., B*, 2012, vols. 113–114, p. 172.
35. Barrera, A., Montoya, J.A., del Angel, P., Navarrete, J., Cano, M.E., Tzompantzi, F., and López-Gaona, A., *J. Phys. Chem. Solids*, 2012, vol. 73, p. 1017.
36. Liu, C., Zhang, C., Sun, S., Liu, K., Hao, S., Xu, J., Zhu, Y., and Li, Y., *ACS Catal.*, 2015, vol. 5, p. 4612.
37. Wu, X., Zhang, L., Weng, D., Liu, S., Si, Z., and Fan, J., *J. Hazard. Mater.*, 2012, vols. 225–226, p. 146.
38. Binet, C., Jádí, A., and Lavalley, J.-C., *J. Chim. Phys.*, 1989, vol. 86, p. 451.
39. Bourguignon, B., Carrez, S., Dragnea, B., and Dubost, H., *Surface Sci.*, 1998, vol. 418, p. 171.
40. Bertarione, S., Scarano, D., Zecchina, A., Johánek, V., Hoffmann, J., Schauer mann, S., Frank, M.M., Libuda, J., Rupprechter, G., and Freund, H.-J., *J. Phys. Chem. B*, 2004, vol. 108, p. 3603.
41. Lear, T., Marshall, R., Antonio Lopez-Sanchez, J., Jackson, S.D., Klapötke, T.M., Bäumer, M., Rupprechter, G., Freund, H.-J., and Lennon, D., *J. Chem. Phys.*, 2005, vol. 123, p. 174706.
42. Clarke, J.K.A., Farren, G.M., and Rubalcava, H.E., *J. Phys. Chem.*, 1967, vol. 71, p. 2376.
43. van Hardeveld, R. and Hartog, F., *Adv. Catal.*, 1972, vol. 22, p. 75.
44. Hadjiivanov, K.I. and Vayssilov, G.N., *Adv. Catal.*, 2002, vol. 47, p. 307.
45. Föttinger, K., Emhofer, W., Lennon, D., and Rupprechter, G., *Top. Catal.*, 2017, vol. 60, p. 1722.
46. Föttinger, K., Schlögl, R., and Rupprechter, G., *Chem. Commun.*, 2008, p. 32.
47. Davydov, A.A., *IK-spektroskopiya v khimii poverkhnosti oksislov* (IR Spectroscopy in the Chemistry of Oxide Surfaces), Novosibirsk: Nauka, 1984.
48. Coq, B., Ferrat, G., and Figueras, F., *J. Catal.*, 1986, vol. 101, p. 434.
49. Pnias, D., Asimidis, P., and Paspaliaris, I., *Hydrometall.*, 2001, vol. 59, p. 15.
50. Yuan, G. and Keane, M.A., *J. Catal.*, 2004, vol. 225, p. 510.
51. de Pedro, Z.M., Diaz, E., Mohedano, A.F., Casas, J.A., and Rodriguez, J.J., *Appl. Catal., B*, 2011, vol. 103, p. 128.
52. Gómez-Sainero, L.M., Seoane, X.L., Fierro, J.L.G., and Arcoya, A., *J. Catal.*, 2002, vol. 209, p. 279.
53. Tarlani, A., Abedini, M., Khabaz, M., and Amini, M.M., *J. Colloid Interface Sci.*, 2005, vol. 292, p. 486.
54. Pizzio, L.R., Cáceres, C.V., and Blanco, M.N., *Appl. Catal., A*, 1998, vol. 167, p. 283.
55. Liu, L., Wang, B., Du, Y., Zhong, Z., and Borgna, A., *Appl. Catal., B*, 2015, vols. 174–175, p. 1.
56. Hoang-Van, C. and Zegaoui, O., *Appl. Catal., A*, 1997, vol. 164, p. 91.
57. Srinivas, S.T., Jhansi Lakshmi, L., Lingaiah, N., Sai Prasad, P.S., and Kanta Rao, P., *Appl. Catal., A*, 1996, vol. 135, p. 201.

*Translated by Andrey Zeigarnik*